

# Measurement of the inclusive semileptonic branching fraction $\mathcal{B}(B_s^0 \rightarrow X^- \ell^+ \nu_\ell)$ at Belle

C. Oswald,<sup>2</sup> P. Urquijo,<sup>2</sup> J. Dingfelder,<sup>2</sup> I. Adachi,<sup>9</sup> H. Aihara,<sup>53</sup> K. Arinstein,<sup>3</sup> D. M. Asner,<sup>42</sup> T. Aushev,<sup>17</sup>  
A. M. Bakich,<sup>47</sup> K. Belous,<sup>16</sup> V. Bhardwaj,<sup>34</sup> B. Bhuyan,<sup>12</sup> A. Bondar,<sup>3</sup> G. Bonvicini,<sup>58</sup> A. Bozek,<sup>38</sup>  
M. Bračko,<sup>27,18</sup> T. E. Browder,<sup>8</sup> P. Chang,<sup>37</sup> V. Chekelian,<sup>28</sup> A. Chen,<sup>35</sup> P. Chen,<sup>37</sup> B. G. Cheon,<sup>7</sup>  
K. Chilikin,<sup>17</sup> R. Chistov,<sup>17</sup> K. Cho,<sup>21</sup> V. Chobanova,<sup>28</sup> S.-K. Choi,<sup>6</sup> Y. Choi,<sup>46</sup> D. Cinabro,<sup>58</sup> J. Dalseno,<sup>28,49</sup>  
Z. Doležal,<sup>4</sup> Z. Drásal,<sup>4</sup> A. Drutskoy,<sup>17,30</sup> D. Dutta,<sup>12</sup> S. Eidelman,<sup>3</sup> S. Esen,<sup>5</sup> H. Farhat,<sup>58</sup> J. E. Fast,<sup>42</sup>  
V. Gaur,<sup>48</sup> N. Gabyshev,<sup>3</sup> S. Ganguly,<sup>58</sup> R. Gillard,<sup>58</sup> Y. M. Goh,<sup>7</sup> B. Golob,<sup>25,18</sup> J. Haba,<sup>9</sup> K. Hayasaka,<sup>33</sup>  
H. Hayashii,<sup>34</sup> Y. Horii,<sup>33</sup> Y. Hoshi,<sup>51</sup> W.-S. Hou,<sup>37</sup> H. J. Hyun,<sup>23</sup> T. Iijima,<sup>33,32</sup> A. Ishikawa,<sup>52</sup> R. Itoh,<sup>9</sup>  
Y. Iwasaki,<sup>9</sup> D. H. Kah,<sup>23</sup> J. H. Kang,<sup>60</sup> E. Kato,<sup>52</sup> T. Kawasaki,<sup>40</sup> C. Kiesling,<sup>28</sup> H. J. Kim,<sup>23</sup> H. O. Kim,<sup>23</sup>  
J. B. Kim,<sup>22</sup> K. T. Kim,<sup>22</sup> M. J. Kim,<sup>23</sup> Y. J. Kim,<sup>21</sup> K. Kinoshita,<sup>5</sup> J. Klucar,<sup>18</sup> B. R. Ko,<sup>22</sup> S. Korpar,<sup>27,18</sup>  
R. T. Kouzes,<sup>42</sup> P. Križan,<sup>25,18</sup> P. Krokovny,<sup>3</sup> B. Kronenbitter,<sup>20</sup> T. Kuhr,<sup>20</sup> T. Kumita,<sup>55</sup> Y.-J. Kwon,<sup>60</sup>  
S.-H. Lee,<sup>22</sup> J. Li,<sup>45</sup> Y. Li,<sup>57</sup> J. Libby,<sup>13</sup> C. Liu,<sup>44</sup> Y. Liu,<sup>5</sup> Z. Q. Liu,<sup>14</sup> D. Liventsev,<sup>9</sup> R. Louvot,<sup>24</sup> O. Lutz,<sup>20</sup>  
D. Matvienko,<sup>3</sup> K. Miyabayashi,<sup>34</sup> H. Miyata,<sup>40</sup> R. Mizuk,<sup>17,30</sup> G. B. Mohanty,<sup>48</sup> A. Moll,<sup>28,49</sup> N. Muramatsu,<sup>43</sup>  
Y. Nagasaka,<sup>10</sup> E. Nakano,<sup>41</sup> M. Nakao,<sup>9</sup> E. Nedelkovska,<sup>28</sup> N. Nellikunnummel,<sup>48</sup> S. Nishida,<sup>9</sup> O. Nitoh,<sup>56</sup>  
T. Nozaki,<sup>9</sup> S. Ogawa,<sup>50</sup> T. Ohshima,<sup>32</sup> S. Okuno,<sup>19</sup> S. L. Olsen,<sup>45</sup> W. Ostrowicz,<sup>38</sup> P. Pakhlov,<sup>17,30</sup> G. Pakhlova,<sup>17</sup>  
H. Park,<sup>23</sup> H. K. Park,<sup>23</sup> T. K. Pedlar,<sup>26</sup> R. Pestotnik,<sup>18</sup> M. Petrič,<sup>18</sup> L. E. Piilonen,<sup>57</sup> M. Prim,<sup>20</sup>  
K. Prothmann,<sup>28,49</sup> M. Ritter,<sup>28</sup> M. Röhrken,<sup>20</sup> M. Rozanska,<sup>38</sup> S. Ryu,<sup>45</sup> H. Sahoo,<sup>8</sup> T. Saito,<sup>52</sup> Y. Sakai,<sup>9</sup>  
S. Sandilya,<sup>48</sup> L. Santelj,<sup>18</sup> T. Sanuki,<sup>52</sup> Y. Sato,<sup>52</sup> O. Schneider,<sup>24</sup> G. Schnell,<sup>1,11</sup> C. Schwanda,<sup>15</sup>  
A. J. Schwartz,<sup>5</sup> K. Senyo,<sup>59</sup> O. Seon,<sup>32</sup> M. E. Sevier,<sup>29</sup> M. Shapkin,<sup>16</sup> C. P. Shen,<sup>32</sup> T.-A. Shibata,<sup>54</sup>  
J.-G. Shiu,<sup>37</sup> B. Shwartz,<sup>3</sup> A. Sibidanov,<sup>47</sup> F. Simon,<sup>28,49</sup> P. Smerkol,<sup>18</sup> Y.-S. Sohn,<sup>60</sup> A. Sokolov,<sup>16</sup>  
E. Solovieva,<sup>17</sup> M. Starič,<sup>18</sup> T. Sumiyoshi,<sup>55</sup> G. Tatishvili,<sup>42</sup> Y. Teramoto,<sup>41</sup> K. Trabelsi,<sup>9</sup> T. Tsuboyama,<sup>9</sup>  
M. Uchida,<sup>54</sup> S. Uehara,<sup>9</sup> T. Uglov,<sup>17,31</sup> Y. Unno,<sup>7</sup> S. Uno,<sup>9</sup> C. Van Hulse,<sup>1</sup> P. Vanhoefer,<sup>28</sup> G. Varner,<sup>8</sup>  
K. E. Varvell,<sup>47</sup> C. H. Wang,<sup>36</sup> M.-Z. Wang,<sup>37</sup> P. Wang,<sup>14</sup> M. Watanabe,<sup>40</sup> Y. Watanabe,<sup>19</sup> K. M. Williams,<sup>57</sup>  
E. Won,<sup>22</sup> H. Yamamoto,<sup>52</sup> Y. Yamashita,<sup>39</sup> C. C. Zhang,<sup>14</sup> Z. P. Zhang,<sup>44</sup> V. Zhilich,<sup>3</sup> and A. Zupanc<sup>20</sup>

(The Belle Collaboration)

<sup>1</sup>University of the Basque Country UPV/EHU, 48080 Bilbao

<sup>2</sup>University of Bonn, 53115 Bonn

<sup>3</sup>Budker Institute of Nuclear Physics SB RAS and Novosibirsk State University, Novosibirsk 630090

<sup>4</sup>Faculty of Mathematics and Physics, Charles University, 121 16 Prague

<sup>5</sup>University of Cincinnati, Cincinnati, Ohio 45221

<sup>6</sup>Gyeongsang National University, Chinju 660-701

<sup>7</sup>Hanyang University, Seoul 133-791

<sup>8</sup>University of Hawaii, Honolulu, Hawaii 96822

<sup>9</sup>High Energy Accelerator Research Organization (KEK), Tsukuba 305-0801

<sup>10</sup>Hiroshima Institute of Technology, Hiroshima 731-5193

<sup>11</sup>Ikerbasque, 48011 Bilbao

<sup>12</sup>Indian Institute of Technology Guwahati, Assam 781039

<sup>13</sup>Indian Institute of Technology Madras, Chennai 600036

<sup>14</sup>Institute of High Energy Physics, Chinese Academy of Sciences, Beijing 100049

<sup>15</sup>Institute of High Energy Physics, Vienna 1050

<sup>16</sup>Institute for High Energy Physics, Protvino 142281

<sup>17</sup>Institute for Theoretical and Experimental Physics, Moscow 117218

<sup>18</sup>J. Stefan Institute, 1000 Ljubljana

<sup>19</sup>Kanagawa University, Yokohama 221-8686

<sup>20</sup>Institut für Experimentelle Kernphysik, Karlsruher Institut für Technologie, 76131 Karlsruhe

<sup>21</sup>Korea Institute of Science and Technology Information, Daejeon 305-806

<sup>22</sup>Korea University, Seoul 136-713

<sup>23</sup>Kyungpook National University, Daegu 702-701

<sup>24</sup>École Polytechnique Fédérale de Lausanne (EPFL), Lausanne 1015

<sup>25</sup>Faculty of Mathematics and Physics, University of Ljubljana, 1000 Ljubljana

<sup>26</sup>Luther College, Decorah, Iowa 52101

<sup>27</sup>University of Maribor, 2000 Maribor

<sup>28</sup>Max-Planck-Institut für Physik, 80805 München

<sup>29</sup>School of Physics, University of Melbourne, Victoria 3010

- <sup>30</sup> *Moscow Physical Engineering Institute, Moscow 115409*  
<sup>31</sup> *Moscow Institute of Physics and Technology, Moscow Region 141700*  
<sup>32</sup> *Graduate School of Science, Nagoya University, Nagoya 464-8602*  
<sup>33</sup> *Kobayashi-Maskawa Institute, Nagoya University, Nagoya 464-8602*  
<sup>34</sup> *Nara Women's University, Nara 630-8506*  
<sup>35</sup> *National Central University, Chung-li 32054*  
<sup>36</sup> *National United University, Miao Li 36003*  
<sup>37</sup> *Department of Physics, National Taiwan University, Taipei 10617*  
<sup>38</sup> *H. Niewodniczanski Institute of Nuclear Physics, Krakow 31-342*  
<sup>39</sup> *Nippon Dental University, Niigata 951-8580*  
<sup>40</sup> *Niigata University, Niigata 950-2181*  
<sup>41</sup> *Osaka City University, Osaka 558-8585*  
<sup>42</sup> *Pacific Northwest National Laboratory, Richland, Washington 99352*  
<sup>43</sup> *Research Center for Electron Photon Science, Tohoku University, Sendai 980-8578*  
<sup>44</sup> *University of Science and Technology of China, Hefei 230026*  
<sup>45</sup> *Seoul National University, Seoul 151-742*  
<sup>46</sup> *Sungkyunkwan University, Suwon 440-746*  
<sup>47</sup> *School of Physics, University of Sydney, NSW 2006*  
<sup>48</sup> *Tata Institute of Fundamental Research, Mumbai 400005*  
<sup>49</sup> *Excellence Cluster Universe, Technische Universität München, 85748 Garching*  
<sup>50</sup> *Toho University, Funabashi 274-8510*  
<sup>51</sup> *Tohoku Gakuin University, Tagajo 985-8537*  
<sup>52</sup> *Tohoku University, Sendai 980-8578*  
<sup>53</sup> *Department of Physics, University of Tokyo, Tokyo 113-0033*  
<sup>54</sup> *Tokyo Institute of Technology, Tokyo 152-8550*  
<sup>55</sup> *Tokyo Metropolitan University, Tokyo 192-0397*  
<sup>56</sup> *Tokyo University of Agriculture and Technology, Tokyo 184-8588*  
<sup>57</sup> *CNP, Virginia Polytechnic Institute and State University, Blacksburg, Virginia 24061*  
<sup>58</sup> *Wayne State University, Detroit, Michigan 48202*  
<sup>59</sup> *Yamagata University, Yamagata 990-8560*  
<sup>60</sup> *Yonsei University, Seoul 120-749*

We report a measurement of the inclusive semileptonic  $B_s^0$  branching fraction in a  $121 \text{ fb}^{-1}$  data sample collected near the  $\Upsilon(5S)$  resonance with the Belle detector at the KEKB asymmetric energy  $e^+e^-$  collider. Events containing  $B_s^{0(*)}\bar{B}_s^{0(*)}$  pairs are selected by reconstructing a tag side  $D_s^+$  and identifying a signal side lepton  $\ell^+$  ( $\ell = e, \mu$ ) that is required to have the same-sign charge to ensure that both originate from different  $B_s^0$  mesons. The  $B_s^0 \rightarrow X^-\ell^+\nu_\ell$  branching fraction is extracted from the ratio of the measured yields of  $D_s^0$  mesons and  $D_s^+\ell^+$  pairs and the known production and branching fractions. The inclusive semileptonic branching fraction is measured to be  $[10.6 \pm 0.5(\text{stat}) \pm 0.4(\text{syst}) \pm 0.6(\text{ext})]\%$ .

PACS numbers: 14.40.Nd, 13.20.He

## INTRODUCTION

Semileptonic decays of  $b$ -flavored mesons constitute a very important class of decays for determination of the elements of the Cabibbo-Kobayashi-Maskawa (CKM) matrix,  $V_{ub}$  and  $V_{cb}$ , and for understanding the origin of  $CP$  violation in the Standard Model (SM). Although semileptonic  $B^0$  and  $B^+$  meson decays have been precisely measured by experiments running at the  $\Upsilon(4S)$  resonance, and have been well studied in theory, experimental information on the decay of the  $B_s^0$  meson is relatively limited. The interest in the physics of the  $B_s^0$  has intensified in recent years, motivated by studies of the dilepton production asymmetry in  $b\bar{b}$  production [1]. Semileptonic  $B_s^0$  decays are used as a normalization mode for various searches for new physics at hadron colliders [2], and in the future with the next generation  $B$  factories. Semilep-

tonic  $B_s^0$  decays also provide an analogous approach to studying the CKM matrix elements and testing theoretical predictions, as meson decays that involve a spectator strange quark can be predicted more accurately than analogous decays with a spectator up or down quark.

An important expectation from heavy quark theory that is exploited in studies of  $B_s^0$  decays is the equality relation, based on  $SU(3)$  symmetry, between the semileptonic decay widths:

$$\Gamma_{\text{SL}}(B_s^0) = \Gamma_{\text{SL}}(B^+) = \Gamma_{\text{SL}}(B^0). \quad (1)$$

The presence of the heavier spectator strange quark introduces, however, some amount of  $SU(3)$  symmetry breaking, as observed in decays of open charm mesons [3]. Theoretical techniques [4, 5] predict that Eq. 1 should hold for  $B_{(s)}$  decays to the percent level, which must be tested in experiment. A measurement of the branching

fraction has been made by the BaBar collaboration, with the result  $\mathcal{B}(B_s \rightarrow X\ell\nu) = [9.5^{+2.5}_{-2.0}(\text{stat})^{+1.1}_{-1.9}(\text{syst})]\%$  [6]. In this paper, we report a measurement of the  $B_s^0 \rightarrow X^-\ell^+\nu_\ell$  branching fractions for  $\ell = e$  and  $\mu$  separately and their weighted average. The measurements are the most precise to date.

## DATA SAMPLE, DETECTOR AND SIMULATION

The data used in this analysis were collected with the Belle detector at the KEKB asymmetric energy  $e^+e^-$  collider [7]. The Belle detector is a large-solid-angle magnetic spectrometer that consists of a silicon vertex detector (SVD), a 50-layer central drift chamber (CDC), an array of aerogel threshold Cherenkov counters (ACC), a barrel-like arrangement of time-of-flight scintillation counters (TOF), and an electromagnetic calorimeter (ECL) comprised of CsI(Tl) crystals located inside a superconducting solenoid coil that provides a 1.5 T magnetic field. An iron flux-return located outside of the coil is instrumented to detect  $K_L^0$  mesons and to identify muons (KLM). The detector is described in detail elsewhere [8].

The results in this paper are based on a  $121\text{ fb}^{-1}$  data sample collected near the  $\Upsilon(5S)$  resonance ( $\sqrt{s} = 10.87\text{ GeV}$ ), which contains  $(7.11 \pm 1.30) \times 10^6 B_s^{0(*)}\bar{B}_s^{0(*)}$  pairs. An additional  $63\text{ fb}^{-1}$  data sample taken at  $\sqrt{s} = 10.52\text{ GeV}$ , below the energy threshold for  $b$ -flavored meson production (off-resonance) is used to subtract background arising from the continuum  $e^+e^- \rightarrow q\bar{q}$  process.

We use Monte Carlo (MC) techniques to separately simulate the production of  $B_{u,d}$  ( $B^+$ ,  $B^0$ ) and  $B_s^0$  mesons at the  $\Upsilon(5S)$  resonance. Events are generated with the EVTGEN event generator [9], and then processed through the detector simulation implemented in GEANT3 [10]. The simulated samples of  $B$ -pair events are equivalent to six times the integrated luminosity of the data. For the simulation of signal semileptonic  $B_s^0$  decays, the lack of exclusive measurements of this system forces us to rely on prior knowledge in the  $B_{u,d}$  systems and employ a variety of phenomenological models. First, we assume the composition of the  $B_s^0$  semileptonic decay width is somewhat analogous to that of the  $B^0$  system [11–13]. We include the following  $B_s^0 \rightarrow X_c\ell\nu$  decay modes in the simulation, with their nominal branching fractions in parentheses:  $X_c = D_s(2.1\%)$ ,  $D_s^*(4.9\%)$ ,  $D_{s0}^*(2317)(0.4\%)$ ,  $D_{s1}(2460)(0.4\%)$ ,  $D_{s1}(2536)(0.7\%)$ , and  $D_{s2}^*(2573)(0.7\%)$ . To simulate these decay modes, we use the ISGW2 quark model [14] for all modes, and an additional model based on heavy quark effective theory (HQET) [15] for the  $B_s \rightarrow D_s^{(*)}\ell\nu$  modes. The form factors for the  $B_s \rightarrow D_s^{(*)}\ell\nu$  modes in the HQET parametrization are taken to be the same as in  $B \rightarrow D^{(*)}\ell\nu$  decays, and the values taken from the Heavy

Flavor Averaging Group [16]. QED final state radiation in semileptonic decays is added using the PHOTOS package [17].

## MEASUREMENT OVERVIEW

Only one fifth of the mesons containing a  $b$ -quark produced near the  $\Upsilon(5S)$  resonance are  $B_s^0$  mesons; the remainder are  $B_{u,d}$  mesons. In this analysis, the relative abundance of  $B_s^0$  mesons is enhanced by reconstructing, or tagging, the CKM-favored  $\bar{B}_s^0 \rightarrow D_s^+$  transition [18], where  $\mathcal{B}(B_s^0 \rightarrow D_s^\pm X) = (93 \pm 25)\%$  [19]. The signal signature is a lepton ( $e^+$ ,  $\mu^+$ ) from the decay of the other  $B_s^0$  in the event. To ensure that this lepton does not originate from the same  $B_s^0$  meson as the reconstructed  $D_s^+$  meson,  $D_s^+\ell^+$  pairs are selected wherein the  $D_s^+$  and  $\ell^+$  have the same electric charge. The quantity obtained in the measurement is the ratio

$$\mathcal{R} = \frac{N_{D_s^+\ell^+}}{N_{D_s^+}} \quad \text{with } \ell = e, \mu, \quad (2)$$

where  $N_{D_s^+}$  and  $N_{D_s^+\ell^+}$  are the efficiency-corrected numbers of  $D_s^+$  and  $D_s^+\ell^+$  pairs in the data. The branching fraction  $\mathcal{B}(B_s^0 \rightarrow X^-\ell^+\nu_\ell)$  is extracted by comparing the ratio  $\mathcal{R}$  to the known production and branching fractions discussed below.

## EVENT SELECTION

### $D_s$ selection

Charged particle tracks are required to originate from a region close to the interaction point by applying the following selections on the impact parameters along the  $z$  axis (opposite the positron beam) and in the perpendicular  $r$ - $\phi$  plane:  $|dz| < 2\text{ cm}$  and  $dr < 0.5\text{ cm}$ . In addition, we demand at least one associated hit in the SVD detector. For pion and kaon candidates, the Cherenkov light yield from the ACC, the time of flight information from the TOF, and the specific ionization  $dE/dx$  from the CDC are required to be consistent with the appropriate mass hypotheses.

Candidate  $D_s^+$  mesons are reconstructed in the cleanest decay mode  $D_s^+ \rightarrow \phi\pi^+$ , with the  $\phi$  resonance reconstructed via  $\phi \rightarrow K^+K^-$ . The reconstructed  $\phi$  and  $D_s^+$  masses are required to lie within  $\pm 8\text{ MeV}$  and  $\pm 65\text{ MeV}$  of the nominal  $\phi$  and  $D_s^+$  masses [20]. The corresponding  $\phi$  selection efficiency is 99%. To suppress misreconstructed  $D_s^+$  mesons, we require  $|\cos\theta_h| > 0.5$ . The helicity angle  $\theta_h$  is defined as the angle between the reconstructed  $D_s^+$  momentum and the  $K^-$  momentum in the  $\phi$  rest frame. Non-resonant  $D_s^+ \rightarrow KK\pi$  decays (such as from S-wave processes) passing the selection criteria are

treated as signal. Correctly reconstructed  $D_s^+$  mesons from  $e^+e^- \rightarrow c\bar{c}$  continuum background typically have high momenta and are suppressed by a requirement on the normalized  $D_s^+$  momentum

$$x(D_s^+) = \frac{p^*(D_s^+)}{p_{\max}^*(D_s^+)} = \frac{p^*(D_s^+)}{\sqrt{s/4 - m(D_s^+)^2}} < 0.5, \quad (3)$$

where  $p^*$  denotes the momentum in the center-of-mass frame of the  $e^+e^-$  beams [21]. Multiple  $D_s^+$  candidates per event are allowed.

### Lepton selection

Each  $D_s^+$  candidate is combined with an electron or muon having the same-sign charge. Electron candidates are identified using the ratio of the energy detected in the ECL to the track momentum, the ECL shower shape, position matching between the track and ECL cluster, the energy loss in the CDC, and the response of the ACC counters. Muons are identified based on their penetration range and transverse scattering in the KLM detector. The polar acceptance regions are  $18^\circ < \theta < 150^\circ$  and  $25^\circ < \theta < 145^\circ$  for electrons and muons, respectively. Leptons are reconstructed with a minimum lepton momentum in the lab frame  $p(\ell^+)$  of 0.6 GeV. Lepton candidates are rejected if they are likely to have originated from  $J/\psi$  decays, using the mass criterion  $|m(\ell^+h^-) - m(J/\psi)| < 5$  MeV, where  $h^-$  is any charged track with a mass hypothesis based on the signal candidate lepton. Electrons that appear to originate from Dalitz  $\pi^0$  decays and from converted photons are removed by requiring  $|m(\ell^+h^-\gamma) - m(\pi^0)| < 32$  MeV and  $|m(\ell^+\ell^-)| < 100$  MeV, respectively. The lepton identification efficiencies multiplied by the geometrical acceptance are 75% (electrons) and 68% (muons). The probabilities that a selected lepton candidate is a misidentified charged kaon or pion are 6% and 19% for electrons and muons, respectively.

The lepton detection efficiencies and misidentification probabilities in the MC simulation are calibrated to data. The calibration factors for the detection efficiencies are obtained from the study of  $\gamma\gamma \rightarrow \ell^+\ell^-$  and  $J/\psi \rightarrow \ell^+\ell^-$ . The misidentification probabilities are determined from  $D^{*+} \rightarrow D^0\pi_{\text{slow}}^+$ ,  $D^0 \rightarrow K^-\pi^+$  decays by studying the electron and muon likelihood of the  $K^-$  and  $\pi^+$  tracks from the  $D^0$ . The pion from the  $D^{*+}$ ,  $\pi_{\text{slow}}^+$ , has a momentum of only a few hundred MeV as it is produced just above the kinematic threshold.

### FIT RESULTS

The number of  $D_s^+$  mesons in data is determined from fits to the  $KK\pi$  mass distribution. The signal shape

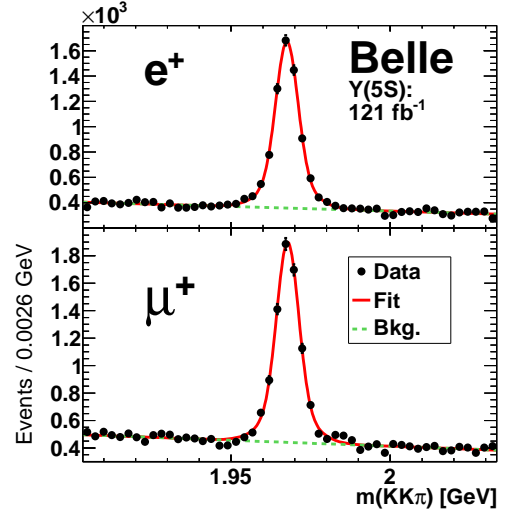


FIG. 1:  $KK\pi$  mass fits to the  $D_s^+\ell^+$  samples collected near the  $\Upsilon(5S)$  resonance. The figure shows the  $KK\pi$  mass for the whole  $p(\ell^+) > 0.6$  GeV range.

used in the fit is modeled as two Gaussian functions with a common mean; the combinatorial background is modeled by a linear function (see Fig. 1). The fit parameters are the normalizations of signal ( $N_{\text{sig}}$ ) and background ( $N_{\text{bkg}}$ ), the slope of the linear function and the parameters of the two Gaussian functions: the common mean, the width of one Gaussian, the ratio of the widths ( $r_\sigma = \sigma_2/\sigma_1$ ) and the ratio of the normalizations ( $r_N$ ).

For the  $N_{D_s^+}$  measurement, the fits are performed in 20 bins of the normalized  $D_s^+$  momentum  $x(D_s^+)$ . The fit results for the parameters  $r_\sigma$  and  $r_N$  are found to be independent of  $x(D_s^+)$ . Figure 2(a) shows the  $D_s^+$  momentum spectra for  $\Upsilon(5S)$  data and off-resonance data. The off-resonance data is scaled with a factor  $S_{\text{cont}} = (\mathcal{L}_{\Upsilon(5S)}/s_{\Upsilon(5S)})/(\mathcal{L}_{\text{off}}/s_{\text{off}})$  to account for the difference in integrated luminosities and the dependence of the quark pair production cross section on the center-of-mass energy  $\sqrt{s}$ . The number of  $D_s^+$  mesons  $N_{D_s^+}$  is obtained by integrating over the region  $x(D_s^+) < 0.5$  and subtracting the continuum background given by the scaled off-resonance distribution. A total of  $[12.42 \pm 0.08(\text{stat})] \times 10^4$   $D_s^+$  mesons are reconstructed, where  $[2.7 \pm 0.1(\text{stat})] \times 10^4$  of these are from continuum processes. This approach is validated by taking the difference between  $\Upsilon(5S)$  and off-resonance data in the control region  $x(D_s^+) > 0.5$ , where only events from the continuum can contribute. The difference is found to be  $-872 \pm 1778$ , consistent with the expectation of zero.

For the  $N_{D_s^+\ell^+}$  measurements, the  $KK\pi$  mass fits are performed in nine bins of lepton momentum in the range  $0.6 \text{ GeV} < p(\ell^+) < 3.1 \text{ GeV}$  (see Figs. 2(b) and 2(c)). The  $D_s^+\ell^+$  samples do not contain enough events to determine all seven fit parameters. Therefore  $r_\sigma$  and  $r_N$



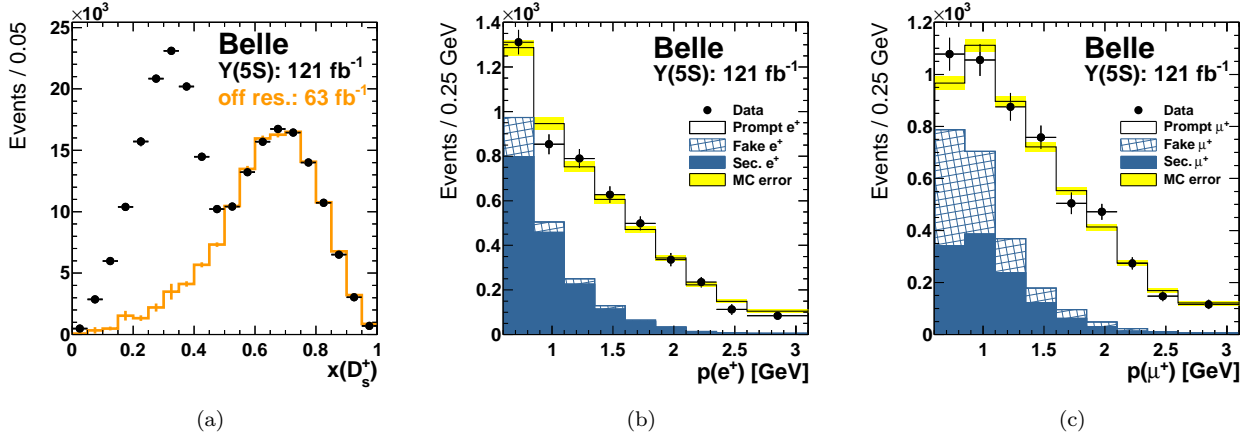


FIG. 2: Momentum spectra obtained from  $KK\pi$  mass fits: (a) In bins of  $x(D_s^+)$  ( $D_s^+$  sample); (b)+(c) In bins of  $p(e^+)$  and  $p(\mu^+)$ , respectively, where continuum backgrounds have been subtracted using off-resonance data ( $D_s^+\ell^+$  sample). The MC uncertainty (yellow) includes both statistical and systematic uncertainties.

are fixed to the values obtained in the  $N_{D_s^+}$  measurement. The remaining parameters, other than  $N_{\text{sig}}$  and  $N_{\text{bkg}}$ , are determined from a fit to the total  $D_s^+\ell^+$  sample without the binning in  $p(\ell^+)$  as shown in Fig. 1. Compared to the  $D_s^+$  sample, the continuum background in the  $D_s^+\ell^+$  sample is suppressed due to the same-sign lepton requirement. The remaining continuum background is subtracted using scaled off-resonance data. The shape difference of the continuum lepton momentum spectra at the  $\Upsilon(5S)$  and in the off-resonance samples is determined from MC simulation and the effect is corrected by a bin-by-bin re-weighting before the subtraction.

A  $\chi^2$  fit to the lepton momentum spectrum is performed with two components: the prompt lepton signal and the remaining  $B_{u,d,s}$  backgrounds, which is the sum of secondary leptons (not coming directly from  $B_{u,d,s}$  decays) and misidentified lepton candidates. The shapes of the signal and  $B_{u,d,s}$  backgrounds are derived from MC simulation. Figures 2(b) and 2(c) show the fit result, and the goodness of the fits is listed in Table I. The numbers of prompt leptons obtained in the fit are corrected for efficiency and geometrical acceptance. The results are extrapolated from the experimental momentum threshold of  $p(\ell^+) > 0.6$  GeV to the full phase space region using MC simulation, where the uncertainty on this acceptance is included in the systematic uncertainties. The signal acceptance in the region  $p(\ell^+) > 0.6$  GeV is 91% for electrons and 92% for muons. Finally, we find  $[4.26 \pm 0.19(\text{stat})] \times 10^3$  and  $[4.76 \pm 0.23(\text{stat})] \times 10^3$  prompt signal electrons and muons, respectively. To determine  $\mathcal{R}$  (Eq. 2), we additionally account for the difference in  $D_s^+$  reconstruction efficiencies between the inclusive  $D_s^+$  and the signal samples  $D_s^+\ell^+$ . These efficiencies take into account the possibility of more than one  $D_s^+ \rightarrow \phi(K^+K^-)\pi^+$  decay per event. The  $D_s^+$  reconstruction efficiencies and the results for  $\mathcal{R}$  are summa-

TABLE I: Measured ratios  $\mathcal{R}$ . The first uncertainty is statistical; the second is systematic. The last row shows the result for the combination of the  $e^+$  and  $\mu^+$  modes and takes into account the correlations.

Mode	Ratio $\mathcal{R} \times 10^{-4}$	$\chi^2/\text{ndf}$	$\epsilon_{D_s^+}(KK\pi)$	$\epsilon_{D_s^+\ell^+}(KK\pi)$
$e$	$428 \pm 20 \pm 13$	6.4 / 7	28.2%	28.7%
$\mu$	$470 \pm 23 \pm 16$	6.7 / 7	28.2%	29.2%
$e, \mu$	$444 \pm 16 \pm 13$	—	—	—

rized in Table I, where the combined result is obtained from the weighted average of the  $e^+$  and  $\mu^+$  modes, taking into account measurement correlations.

## SYSTEMATIC UNCERTAINTIES ON $\mathcal{R}$

The systematic uncertainties on the ratio  $\mathcal{R}$  are divided into four categories: detector effects, fitting procedure, background modeling and signal modeling. They are discussed in turn below, and are given as relative uncertainties.

Numerous potential systematic uncertainties that relate to the reconstruction of the  $D_s^+$  ultimately cancel in the ratio; these include uncertainties associated with kaon and pion reconstruction. The uncertainty on the calibration of the electron (muon) identification is 0.7% (1.4%). The uncertainty on the lepton misidentification is below 0.1%. Another 0.35% uncertainty is added for the reconstruction efficiency of the lepton track. The statistical uncertainty of the efficiencies  $\epsilon_{D_s^+e^+}(KK\pi)$  and  $\epsilon_{D_s^+\mu^+}(KK\pi)$  is 0.8%.

Uncertainties in the modeling of the  $KK\pi$  mass shape cancel in the ratio  $\mathcal{R}$ . The shape parameters fixed in the  $N_{D_s^+\ell^+}$  fits are each varied by one standard deviation and the variations on the fit results are added in quadrature

to determine the systematic uncertainty. This results in an uncertainty of 2.0% (2.2%) for electrons (muons).

The scale factor  $S_{\text{cont}}$  for the off-resonance data and the correction of the off-resonance lepton momentum spectrum add uncertainties of 0.4% and 1%, respectively. The knowledge of the composition of the fit component containing the combined background from secondary leptons and misidentified lepton candidates is limited by the precision of the measurements of  $B_s^0$  branching fractions, which is estimated to be of the order of 30%. Hence, the yields of secondary leptons from  $D_{u,d,s}$ , from  $\tau$  and from other decays, as well as the rate of misidentified leptons are scaled by  $\pm 30\%$  and the variation of  $\mathcal{R}$  is taken as systematic uncertainty, giving 1.0% (1.5%) for electrons (muons).

For the signal model, since most of the exclusive modes have not been measured, the shape uncertainty is estimated as the full difference between the result obtained with HQET and with the ISGW2 model where applicable. For electrons (muons), the obtained uncertainty is 0.7% (0.6%). Since the background from  $B_{u,d}$  decays is expected to contribute less than 20% of the measured semileptonic yield and the semileptonic width of  $B_{u,d}$  decays has been studied in more detail, the shape uncertainties are found to be negligible compared to  $B_s^0$  decays.

The uncertainty due to the composition of the semileptonic width is evaluated by varying the normalization of each mode by  $\pm 30\%$  and adding the uncertainties in quadrature. The resulting uncertainties on  $\mathcal{R}$  are 1.0% and 1.1% for electrons and muons, respectively. Due to the inclusiveness of the analysis, the total uncertainty on the signal lepton acceptance is only 0.3%.

The total systematic uncertainty on  $\mathcal{R}$  is calculated by summing the above uncertainties in quadrature. It is found to be 3.0% (2.7%) for electrons and 3.5% (2.8%) for muons, where the values in parentheses are the fully correlated errors between both modes. Taking these correlations into account, the total systematic uncertainty on the combined value of  $\mathcal{R}$  is 3.0%.

## EXTRACTION OF THE BRANCHING FRACTION

The extraction of the  $B_s^0 \rightarrow X^- \ell^+ \nu_\ell$  branching fraction is based on a prediction of the measured ratio  $\mathcal{R}$  and includes the estimation of the background from  $B_{u,d}$  decays. This approach is based on the calculation of the number of same-sign lepton pairs  $\ell^+ \ell^+$  in  $\Upsilon(5S)$  decays discussed in Ref. [22]. The measured yields  $N_\zeta$  (where  $\zeta = D_s^+, D_s^+ \ell^+$ ) contain a contribution

from  $B_s^0$  decays  $\mathcal{N}_\zeta(B_s^{(*)} \bar{B}_s^{(*)})$  and from  $B_{u,d}$  background  $\mathcal{N}_\zeta(B_{u,d}^{(*)} \bar{B}_{u,d}^{(*)}(\pi))$ :

$$\mathcal{R} = \frac{\mathcal{N}_{D_s^+ \ell^+}(B_s^{(*)} \bar{B}_s^{(*)}) + \mathcal{N}_{D_s^+ \ell^+}(B_{u,d}^{(*)} \bar{B}_{u,d}^{(*)}(\pi))}{\mathcal{N}_{D_s^+}(B_s^{(*)} \bar{B}_s^{(*)}) + \mathcal{N}_{D_s^+}(B_{u,d}^{(*)} \bar{B}_{u,d}^{(*)}(\pi))}. \quad (4)$$

The total number of produced  $b$ -quark pairs,  $N_{b\bar{b}}$ , cancels in the ratio. Pairs of  $b\bar{b}$  quarks produced near the  $\Upsilon(5S)$  resonance hadronize in pairs of  $B_{u,d}$  mesons with a probability of  $f_{ud} = f_u + f_d$ , where  $f_u = \mathcal{B}(\Upsilon(5S) \rightarrow B^\pm X)/2 = (36.1 \pm 3.2)\%$  and  $f_d = \mathcal{B}(\Upsilon(5S) \rightarrow B^0 X)/2 = (38.5 \pm 4.2)\%$  [23].  $B_s^0$  pairs are formed with a probability of  $f_s = (19.9 \pm 3.0)\%$  [20]. The remaining contribution to the  $\Upsilon(5S) \rightarrow b\bar{b}$  decay width are bottomonium resonances, but no subsequent decays of these resonances to  $D_s^+$  mesons have been observed so far. The contribution from bottomonium is assumed to be negligible in the ratio  $\mathcal{R}$ , and neglected in the calculations.

The production of  $B_{u,d}$  mesons near the  $\Upsilon(5S)$  center-of-mass energy is divided in three classes [23]: two-body decays  $B_{u,d}^{(*)} \bar{B}_{u,d}^{(*)}$ , three-body decays with an additional pion  $B_{u,d}^{(*)} \bar{B}_{u,d}^{(*)} \pi$  and the initial state radiation (ISR) process  $e^+ e^- \rightarrow \gamma_{\text{ISR}} \Upsilon(4S) \rightarrow \gamma_{\text{ISR}} B_{u,d} \bar{B}_{u,d}$ . The fractions of the different two-body production mechanisms are given by the parameters  $F_{B\bar{B}}$ ,  $F_{B^* \bar{B}}$  and  $F_{B^* \bar{B}^*}$ , and their sum is denoted by  $F_2$ . The fraction of three-body decays is  $(f_{ud} - F_2) \cdot F'_3$ , where  $F'_3 = F'_{B\bar{B}\pi} + F'_{B^* \bar{B}\pi} + F'_{B^* \bar{B}^* \pi}$ . The remainder  $(f_{ud} - F_2) \cdot (1 - F'_3)$  is attributed to the ISR process. From isospin symmetry, one can deduce that one-third of the three-body decay modes are  $B^{(*)} B^{(*)} \pi^0$  and  $B^{0(*)} \bar{B}^{0(*)} \pi^0$ , with the remainder being  $B^{(*)} \bar{B}^{0(*)} \pi^-$  or  $B^{-(*)} B^{0(*)} \pi^+$ .

The mixing probability  $\chi_q^{(\mathcal{C})}$  of a pair of  $B_q^0$  mesons ( $q = d, s$ ) depends on  $x_q = \Delta m_{B_q^0} / \Gamma_{B_q^0}$  and the  $\mathcal{C}$  eigenstate in which the pair is produced:

$$\chi_q^{(+)} = \frac{x_q^2(3 + x_q^2)}{2(1 + x_q^2)^2} \quad \text{and} \quad \chi_q^{(-)} = \frac{x_q^2}{2(1 + x_q^2)}. \quad (5)$$

In contrast to  $B^0$  mesons, where  $x_d = 0.770 \pm 0.008$  [20],  $x_s = 26.49 \pm 0.29$  [20] is so large for  $B_s^0$  mesons that the difference between even and odd  $\mathcal{C}$  eigenstates can be neglected. We use the approximation  $\chi_s = (1 - \chi_s) = 0.500 \pm 0.001$ . For  $B^0$  produced together with a charged  $B^-$  meson, the mixing probability is the same as for  $\mathcal{C} = -1$ . With this information, the contributions  $\mathcal{N}$  to the yields from each  $b$ -flavored meson production mode can be calculated:

$$\mathcal{N}_{D_s^+}(B_s^{(*)} \bar{B}_s^{(*)}) = N_{b\bar{b}} \cdot 2 \cdot f_s \cdot \mathcal{B}(B_s^0 \rightarrow D_s^\pm X), \quad (6)$$

$$\mathcal{N}_{D_s^+}(B_{u,d}^{(*)} \bar{B}_{u,d}^{(*)}(\pi)) = N_{b\bar{b}} \cdot [2 \cdot f_d \cdot \mathcal{B}(B^0 \rightarrow D_s^\pm X) + 2 \cdot f_u \cdot \mathcal{B}(B^+ \rightarrow D_s^\pm X)], \quad (7)$$

$$\mathcal{N}_{D_s^+ \ell^+}(B_s^{0(*)} \bar{B}_s^{0(*)}) = N_{b\bar{b}} \cdot 2 \cdot f_s \cdot \mathcal{B}(B_s^0 \rightarrow X^- \ell^+ \nu_\ell) \cdot (1 - \chi_s) \cdot \mathcal{B}(B_s^0 \rightarrow D_s^\pm X). \quad (8)$$

TABLE II: Production of  $B_{u,d}$  mesons at the  $\Upsilon(5S)$  center-of-mass energy. The specified modes contribute with a fraction  $F$  to the total amount of  $b\bar{b}$  pairs. For the modes with  $B^{0(*)}$  mesons, the  $\mathcal{C}$  eigenstate is given.

Mode	Production Fraction	$\mathcal{C}$
$B^0\bar{B}^0$	$f_d/f_{ud} \cdot F_{B\bar{B}}$	—
$B^{0*}\bar{B}^0$	$f_d/f_{ud} \cdot F_{B^*\bar{B}}$	+
$B^{0*}\bar{B}^{0*}$	$f_d/f_{ud} \cdot F_{B^*\bar{B}^*}$	—
$B^{+(*)}B^{-(*)}$	$f_u/f_{ud} \cdot F_2$	—
$B^0\bar{B}^0\pi^0$	$f_d/f_{ud} \cdot 1/3 \cdot (f_{ud} - F_2) \cdot F'_{B\bar{B}\pi}$	—
$B^{0*}\bar{B}^0\pi^0$	$f_d/f_{ud} \cdot 1/3 \cdot (f_{ud} - F_2) \cdot F'_{B^*\bar{B}\pi}$	+
$B^{0*}\bar{B}^{0*}\pi^0$	$f_d/f_{ud} \cdot 1/3 \cdot (f_{ud} - F_2) \cdot F'_{B^*\bar{B}^*\pi}$	—
$B^{+(*)}B^{-(*)}\pi^0$	$f_u/f_{ud} \cdot 1/3 \cdot (f_{ud} - F_2) \cdot F'_3$	—
$B^{0(*)}B^{-(*)}\pi^+$	$2/3 \cdot (f_{ud} - F_2) \cdot F'_3$	—
$B^0\bar{B}^0\gamma_{\text{ISR}}$	$f_d/f_{ud} \cdot (f_{ud} - F_2) \cdot (1 - F'_3)$	—
$B^+B^-\gamma_{\text{ISR}}$	$f_u/f_{ud} \cdot (f_{ud} - F_2) \cdot (1 - F'_3)$	—

The factor of two takes into account the possibility that the reconstructed  $D_s^+$  meson can stem from either of the two  $b$ -flavored mesons. The contributions from  $B_{u,d}$  mesons,  $\mathcal{N}_{D_s^+\ell^+}(B^{0*}\bar{B}^0\pi)$ , are sensitive to numerous possible production modes, as summarized in Table II; the formula for the  $\Upsilon(5S) \rightarrow B^{0*}\bar{B}^0\pi$  mode is shown as an example:

$$\begin{aligned} \mathcal{N}_{D_s^+\ell^+}(B^{0*}\bar{B}^0\pi) &= N_{b\bar{b}} \cdot 2 \cdot (f_d/f_{ud}) \cdot \frac{1}{3} \cdot (f_{ud} - F_2) \cdot \\ &F'_{B^*\bar{B}\pi} \cdot \mathcal{B}(B^0 \rightarrow X\ell^+\nu_\ell) \cdot [\chi_d^{(+)} \cdot \mathcal{B}(B^0 \rightarrow D_s^+X) + \\ &(1 - \chi_d^{(+)}) \cdot \mathcal{B}(B^0 \rightarrow D_s^-X)] . \end{aligned} \quad (9)$$

The parameters used to calculate the  $\mathcal{N}$  terms are summarized in Table III. Equation 4 is solved for  $\mathcal{B}(B_s^0 \rightarrow X^-\ell^+\nu_\ell)$ , which is the only unknown quantity. The uncertainties on  $\mathcal{B}(B_s^0 \rightarrow X^-\ell^+\nu_\ell)$  from the external parameters are obtained by varying each of them in turn by their uncertainties; for asymmetric uncertainties, the larger one is used. The external parameters are treated as if they were uncorrelated. The correlations between the ratio  $\mathcal{R}$  and the external parameters measured at Belle are negligible.

## RESULTS AND DISCUSSION

We obtain the following values for the semileptonic branching fraction  $\mathcal{B}(B_s^0 \rightarrow X^-\ell^+\nu_\ell)$ :

$$\begin{aligned} \ell = e & \quad [10.1 \pm 0.6(\text{stat}) \pm 0.4(\text{syst}) \pm 0.6(\text{ext})]\% , \\ \ell = \mu & \quad [11.3 \pm 0.7(\text{stat}) \pm 0.5(\text{syst}) \pm 0.7(\text{ext})]\% , \\ \ell = e, \mu & \quad [10.6 \pm 0.5(\text{stat}) \pm 0.4(\text{syst}) \pm 0.6(\text{ext})]\% . \end{aligned}$$

The last branching fraction is the combination of the electron and muon mode measurements. Our result is consis-

TABLE III: Central values used for the extraction of the branching fraction  $\mathcal{B}$ . The relative systematic uncertainty  $|\Delta\mathcal{B}/\mathcal{B}|$  is given for the combined measurement. Parameter values are taken from Ref. [20] unless otherwise stated.

Parameter	Value	$ \Delta\mathcal{B}/\mathcal{B} [\%]$
$f_u = \mathcal{B}(\Upsilon(5S) \rightarrow B^\pm X)/2$	$(36.1 \pm 3.2)\%$ [23]	0.8
$f_d = \mathcal{B}(\Upsilon(5S) \rightarrow B^0 X)/2$	$(38.5 \pm 4.2)\%$ [23]	0.6
$f_s$	$(19.9 \pm 3.0)\%$	2.4
$\mathcal{B}(B_s \rightarrow D_s^\pm X)$	$(93 \pm 25)\%$ [19]	4.4
$\mathcal{B}(B^+ \rightarrow D_s^+ X)$	$(7.9 \pm 1.4)\%$	2.2
$\mathcal{B}(B^0 \rightarrow D_s^+ X)$	$(10.3 \pm 2.1)\%$	1.7
$\mathcal{B}(B^0 \rightarrow D_s^- X)$	$(1.5 \pm 0.8)\%$ [24]	1.1
$\mathcal{B}(B^+ \rightarrow D_s^- X)$	$(1.1 \pm 0.4)\%$	0.9
$\mathcal{B}(B^0 \rightarrow X\ell^+\nu_\ell)$	$(10.33 \pm 0.28)\%$	0.4
$\mathcal{B}(B^+ \rightarrow X\ell^+\nu_\ell)$	$(10.99 \pm 0.28)\%$	0.1
$F_{B^*\bar{B}^*}$	$(38.1 \pm 3.4)\%$	0.1
$F_{B^*\bar{B}}$	$(13.7 \pm 1.6)\%$	0.1
$F_{B\bar{B}}$	$(5.5 \pm 1.6)\%$	0.0
$F'_{B^*\bar{B}^*\pi}$	$(5.9 \pm 7.8)\%$ [23]	0.1
$F'_{B^*\bar{B}\pi}$	$(41.6 \pm 12.1)\%$ [23]	0.2
$F'_{B\bar{B}\pi}$	$(0.2 \pm 6.8)\%$ [23]	0.0
$x_d$	$0.771 \pm 0.008$	0.1
$\chi_s$	$0.500 \pm 0.001$	0.2

TABLE IV: Relative uncertainties on the branching fraction  $\mathcal{B}(B_s^0 \rightarrow X\ell^+\nu_\ell)$  for the electron and muon mode, and their combination.

Uncertainty [%]	$e$	$\mu$	$e, \mu$
Statistical	5.7	6.0	4.2
$\ell$ reconstruction, ID and fake rate	0.9	1.7	1.0
$D_s$ reconstruction efficiencies	1.0	1.0	0.7
Shape error in $KK\pi$ mass fits	2.4	2.6	2.4
Continuum background estimation	1.3	1.2	1.3
Secondary and fake $\ell$ bkg. composition	1.8	1.8	1.3
Model of the semileptonic width	1.5	1.4	1.4
External parameters	5.8	6.3	6.0

tent with the measurement in Ref. [6] and substantially improves on both the statistical and systematic precision.

Table IV summarizes the uncertainties of the branching fractions. The dominant uncertainty arises from the external parameters. This is typical for almost any  $B_s^0$  absolute branching fraction measurement where the  $B_s^0$  production rate near the  $\Upsilon(5S)$  resonance has to be estimated. In this measurement, the critical parameters  $f_s$  and  $\mathcal{B}(B_s \rightarrow D_s^\pm X)$  appear in the numerator and denominator of the ratio  $\mathcal{R}$  and therefore the respective uncertainties partially cancel. The measurement of the ratio  $\mathcal{R}$  is kept independent of the extraction of  $\mathcal{B}(B^0 \rightarrow X^-\ell^+\nu_\ell)$ , in order to facilitate the update of the branching fraction when the precision of external measurements improves.

Using the well measured lifetimes of the  $B_s^0$  and  $B^0$  mesons, and  $\mathcal{B}(B^0 \rightarrow X^-\ell^+\nu_\ell)$  [20], the inclusive semileptonic width of the  $B_s^0$  is determined to be  $\Gamma_{\text{SL}}(B_s^0) = (1.04 \pm 0.09) \cdot \Gamma_{\text{SL}}(B^0)$  which is consistent

with the theoretical expectation [4, 5]. This level of precision is already an important test of the theoretical description of semileptonic  $B_s^0$  decays. To fully understand  $SU(3)$  symmetry breaking effects, the heavy quark parameters of semileptonic  $B_s^0$  decays must be measured directly. This can be achieved through the analysis of spectral moments, although it will require full reconstruction techniques only feasible at a next generation flavor factory.

### SUMMARY

We measured the inclusive semileptonic  $B_s^0$  branching fraction  $\mathcal{B}(B_s^0 \rightarrow X^- \ell^+ \nu_\ell) = [10.6 \pm 0.5(\text{stat}) \pm 0.4(\text{syst}) \pm 0.6(\text{ext})]\%$ . This is the most precise measurement to date and in agreement with the previous measurement [6] and theoretical expectations [4, 5].

### ACKNOWLEDGEMENTS

We thank the KEKB group for the excellent operation of the accelerator; the KEK cryogenics group for the efficient operation of the solenoid; and the KEK computer group, the National Institute of Informatics, and the PNNL/EMSL computing group for valuable computing and SINET4 network support. We acknowledge support from the Ministry of Education, Culture, Sports, Science, and Technology (MEXT) of Japan, the Japan Society for the Promotion of Science (JSPS), and the Tau-Lepton Physics Research Center of Nagoya University; the Australian Research Council and the Australian Department of Industry, Innovation, Science and Research; the National Natural Science Foundation of China under contract No. 10575109, 10775142, 10875115 and 10825524; the Ministry of Education, Youth and Sports of the Czech Republic under contract No. LA10033 and MSM0021620859; the Department of Science and Technology of India; the Istituto Nazionale di Fisica Nucleare of Italy; the BK21 and WCU program of the Ministry Education Science and Technology, National Research Foundation of Korea, and GSDC of the Korea Institute of Science and Technology Information; the Polish Ministry of Science and Higher Education; the Ministry of Education and Science of the Russian Federation and the Russian Federal Agency for Atomic Energy; the Slovenian Research Agency; the Swiss National Science Foundation; the National Science Council and the Ministry of Education of Taiwan; and the U.S. Department of Energy and the National Science Foundation. This work

is supported by a Grant-in-Aid from MEXT for Science Research in a Priority Area (“New Development of Flavor Physics”), and from JSPS for Creative Scientific Research (“Evolution of Tau-lepton Physics”).

- 
- [1] V. Abazov *et al.* [D0 Collaboration], Phys. Rev. D **82**, 032001 (2010).
  - [2] R. Aaij *et al.* [LHCb Collaboration], Phys. Rev. D **85**, 032008 (2012).
  - [3] D. M. Asner *et al.* [CLEO Collaboration], Phys. Rev. D **81**, 052007 (2010).
  - [4] M. Gronau and J. L. Rosner, Phys. Rev. D **83**, 034025 (2011).
  - [5] I. I. Bigi, T. Mannel and N. Uraltsev, JHEP **1109**, 012 (2011).
  - [6] J. P. Lees *et al.* [BaBar Collaboration], Phys. Rev. D **85**, 011101 (2012).
  - [7] S. Kurokawa and E. Kikutani, Nucl. Instrum. Meth. A **499**, 1 (2003), and other papers included in this volume.
  - [8] A. Abashian *et al.*, Nucl. Instrum. Meth. A **479**, 117 (2002).
  - [9] D. J. Lange, Nucl. Instrum. Meth. A **462**, 152 (2001).
  - [10] R. Brun *et al.*, GEANT 3.21 CERN Report DD/EE/84-1, (1984).
  - [11] J. A. Bailey *et al.*, Phys. Rev. D **85**, 114502 (2012). Erratum-ibid. D **86**, 039904 (2012).
  - [12] X. J. Chen, H. F. Fu, C. S. Kim and G. L. Wang, J. Phys. G **39**, 045002 (2012).
  - [13] G. Li, F.-L. Shao and W. Wang, Phys. Rev. D **82**, 094031 (2010).
  - [14] D. Scora and N. Isgur, Phys. Rev. D **52**, 2783 (1995).
  - [15] I. Caprini, L. Lellouch and M. Neubert, Nucl. Phys. B **530**, 153 (1998).
  - [16] Y. Amhis *et al.* [Heavy Flavor Averaging Group], [arXiv:1207.1158](https://arxiv.org/abs/1207.1158) [hep-ex].
  - [17] E. Barberio and Z. Was, Comput. Phys. Commun. **79**, 291 (1994).
  - [18] Throughout this paper, the inclusion of the charge conjugate mode decay is implied unless otherwise stated.
  - [19] We interpret the average  $\mathcal{B}(B_s^0 \rightarrow D_s^\pm X) = (93 \pm 25)\%$  from Ref. [16] as a multiplicity (*i.e.*, the value can be greater than one), not as a branching fraction  $\mathcal{B}(B_s^0 \rightarrow D_s^\pm X)$ .
  - [20] J. Beringer *et al.* [Particle Data Group], Phys. Rev. D **86**, 010001 (2012).
  - [21] Throughout this paper, the convention  $c = 1$  is used.
  - [22] R. Louvot, “Study of  $B_s^0$ -meson production and measurement of  $B_s^0$  decays into a  $D_s^{(*)}$  and a light meson in  $e^+e^-$  collisions at  $\sqrt{s} = 10.87$  GeV,” PhD thesis #5213, EPFL (2012).
  - [23] A. Drutskoy *et al.* [Belle Collaboration], Phys. Rev. D **81**, 112003 (2010).
  - [24] B. Aubert *et al.* [BABAR Collaboration], Phys. Rev. D **75**, 072002 (2007).